Neocortex Patterning by the Secreted Signaling Molecule FGF8

Tomomi Fukuchi-Shimogori and Elizabeth A. Grove*

A classic model proposes that the mammalian neocortex is divided into areas early in neurogenesis, but the molecular mechanisms that generate the area map have been elusive. Here we provide evidence that FGF8 regulates development of the map from a source in the anterior telencephalon. Using electroporation-mediated gene transfer in mouse embryos, we show that augmenting the endogenous anterior FGF8 signal shifts area boundaries posteriorly, reducing the signal shifts them anteriorly, and introducing a posterior source of FGF8 elicits partial area duplications, revealed by ectopic somatosensory barrel fields. These findings support a role for FGF signaling in specifying positional identity in the neocortex.

The mammalian cerebral cortex is divided into anatomically and functionally distinct areas, forming a species-specific area map across the cortical sheet (*1*). Identifying the mechanisms that generate the map is thus key to understanding the development of cortical function and may clarify how different maps are generated in different species. In a classic model, an area "protomap" is set up in the proliferative cell layer of the neocortex (*2*). Recently, it has been proposed that the protomap could be specified by signaling proteins secreted from nearby signaling centers, a patterning strategy used elsewhere in the embryo (*3*–*7*). Candidate sources have been identified of proteins implicated in vertebrate and invertebrate embryonic patterning, including members of the fibroblast growth factor (FGF), Wingless-Int (WNT), and bone morphogenetic protein (BMP) families (*8*–*11*). In this study we sought direct evidence that such a patterning strategy is used to generate the neocortical area map.

Patterning roles for the FGF family member FGF8 have been reported for the first branchial arch, the midbrain, and the initial formation of the telencephalon (*10*, *12*–*16*). Indicating that FGF8 could also be a regulator of anterior/posterior (A/P) neocortical pattern, FGF8 is expressed close to the anterior pole of the neocortical primordium (*4*, *8*, *17*) (Fig. 1B), and the primordium itself shows A/P graded expression of genes encoding FGF receptors FGFR1, 2, and 3 (*18*). To test this hypothesis, we analyzed the effects on the area map of augmenting the anterior FGF8 source in the embryonic mouse cerebrum, sequestering endogenous FGF8 with a soluble FGF receptor construct, or introducing a second, posterior source of FGF8. To direct gene misexpression to select sites in a single cerebral hemisphere, we adapted the method of microelectroporation (*19*, *20*) for gene transfer in mice in utero (Fig. 1A). Mice are born normally and can be analyzed at any age, making this method a useful adjunct to the generation of genetically engineered mice, which often do not survive past birth.

Expanding the anterior FGF8 source shifts cortical area boundaries posteriorly. FGF8 was initially overexpressed in the anterior cortical primordium, just posterior to the endogenous source (Fig. 1C). We predicted that augmenting the endogenous FGF8 signal in this way would distort the area map along the A/P axis. Embryos were electroporated at embryonic day 11.5 (E11.5)—early in neocortical neurogenesis, before neocortical area identity is determined (*21*–*23*)—and analyzed postnatally. At postnatal day 0 (P0), several neocortical gene-expression patterns indicate emerging area boundaries along the A/P axis, although true cytoarchitectonic boundaries are not yet visible. *EphrinA5* encodes an Eph ligand and is expressed most strongly in presumptive somatosensory cortex; *sFrp2* encodes secreted frizzled related protein 2 and is expressed anterior to *EphrinA5*; and *Rzr-beta* encodes an orphan nuclear receptor and is expressed in both domains (*4*, *5*, *24*) (Fig. 2, A to C). As predicted, in *Fgf8*-electroporated hemispheres (n = 6), these expression domains shift in a coordinated manner toward the posterior pole of the cortex (Fig. 2, D to F). By P6 in the mouse, a true area boundary, defined by cytoarchitecture (*1*), appears between primary somatosensory and motor areas (Fig. 2G). In *Fgf8*-electroporated hemispheres analyzed at P6 (n = 10), this area boundary, also distinguished by transitions in gene expression (*4*), is shifted posteriorly (Fig. 2, J to L).

For a global view of the changes in the area map caused by anterior FGF8 overexpression, we examined expression of the type II classic cadherins, *Cadherin-6* (*Cdh6*) and *Cadherin-8* (*Cdh8*), in P6 brain whole mounts. At this age, differential expression of *Cdh6* and *Cdh8* distinguishes a frontal domain composed of cingulate, prefrontal, and motor areas; a parietal domain that contains somatosensory areas; and an occipital domain that includes visual areas (*5*, *6*, *25*) (Fig. 3, A to C). In *Fgf8*-electroporated P6 left hemispheres (n = 12), the frontal domain is expanded at the apparent expense of parietal and occipital domains, which are shrunken and shifted back (Fig. 3, B and D). Thus, consistent with the hypothesis that FGF8 regulates pattern along the A/P axis, augmenting the endogenous FGF8 source results in an expansion of an anterior neocortical domain with a concomitant shifting and shrinkage of more posterior areas.

Area boundary shifts are not due to a simple growth effect. FGF8 can regulate cell proliferation in vivo and shows transforming potential in vitro (*15*, *26*–*28*). However, the expansion of anterior neocortex seen with FGF8 overexpression is not a simple growth effect. Although the anterior domain expands, more posterior domains contract, so that *Fgf8*-electroporated hemispheres do not show gross overall increases in A/P length compared with control hemispheres (Fig. 2, A to F, and Fig. 3, B and D). By contrast, anterior overexpression of another growth factor, WNT3A, implicated in hippocampal cell proliferation (*29*), expands the frontal *Cdh8*-expressing cortical domain by causing a marked overgrowth at the frontal pole of the hemisphere (n = 5) (Fig. 3G). Anterior overexpression of FGF8 appears, instead, to shift the position of areas within the hemisphere.

Reducing the endogenous FGF8 signal shifts cortical area boundaries anteriorly. To test whether an endogenous FGF signal coordinates the area map, we expressed a soluble form of FGFR3c (sFGFR3) close to the anterior FGF8 source. FGFR3c is a high-affinity FGF8 receptor isoform, and the soluble form is expected to sequester endogenous FGF8, and potentially other FGF family members, blocking their ability to activate endogenous receptors (*14*, *30*, *31*). *sFGFR3*-electroporated hemispheres show no gross decrease in overall size, but the frontal *Cdh8*-expressing cortical domain shrinks (n = 7) (Fig. 3F) and other gene expression domains shift anteriorly (*32*). These observations and others cited below indicate that an endogenous FGF signal regulates neocortical pattern and that it is still active at E11.5.

A signal feature of neocortical sensory and motor areas is that they contain topographic, functional representations of the body. We examined the effects of augmenting or reducing FGF8 signaling on this feature of area identity, focusing on the modular organization of primary somatosensory cor-

Department of Neurobiology, Pharmacology and Physiology, University of Chicago, Chicago, IL 60637, USA.

*To whom correspondence should be addressed. E-mail: egrove@drugs.bsd.uchicago.edu

tex (S1). In rodent S1, an array of barrels reflects the pattern of whiskers on the animal's snout, each barrel innervated by thalamocortical axons carrying sensory information from a single whisker (*33*–*35*). The barrel fields are normally located in a central position along the A/P axis of the neocortex (Fig. 4A). Anterior electroporation of *Fgf8* shifts the fields posteriorly and compresses them (n = 9) (Fig. 4, D and E), whereas electroporation of *sFGFR3* shifts them anteriorly (n = 12) (Fig. 4, G and H). Suggesting that FGF signaling regulates neocortical patterning not only at a broad scale, but also at a fine scale, the latter manipulation also skews the outline of both barrel subfields and individual barrels, elongating them along their A/P axis (compare Fig. 4, B and H).

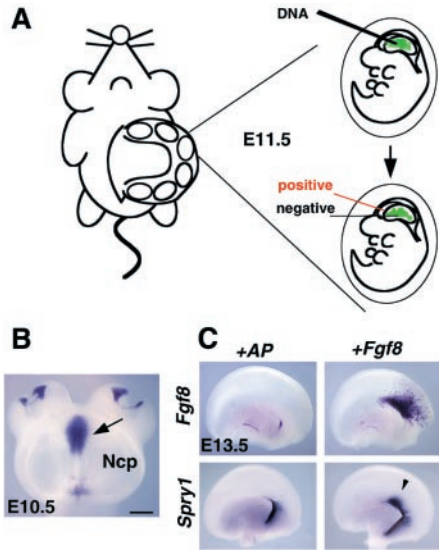

Fig. 1. (**A**) In utero electroporation-mediated gene transfer used to modify FGF8 signaling in mouse cortical primordium. Laparotomies were performed at E11.5 (*38*), and embyros were visualized through the uterus with a fiber optic light source. Plasmid DNA (0.5 to 1.0 μg/μl) (*39*) was mixed with 1% fast green (Sigma) and injected into the left cerebral ventricle of each embryo through a glass capillary. A fine tungsten negative electrode and a platinum positive electrode were inserted into the left and right hemispheres, respectively, and a series of three square-wave current pulses (7 to 10 V, 100 ms) were delivered, resulting in gene transfection into the medial wall of the left hemisphere. The surgical incision was closed and embryos were allowed to develop in utero, with 50 to 60% survival beyond birth (*40*). (**B**) An untreated E10.5 forebrain viewed from the dorsal side, anterior to the top, processed for whole-mount in situ hybridization (*11*). *Fgf8* is expressed in the anteromedial telencephalon in continuity with the neocortical primordium (Ncp, arrow). Other sites of expression, separated from the cortical primordium, are the face primordia and diencephalon. (**C**) E13.5 left cerebral hemispheres viewed from the medial face, anterior to the right, electroporated with *Alkaline Phosphatase* (*AP*+) or *Fgf8* (*Fgf8*+) constructs at E11.5. +*AP* hemispheres display limited endogenous expression of *Fgf8* and *Sprouty1* (*Spry1*), a rapid response gene in the FGF signaling pathway (*41*), by this age. +*Fgf8* hemispheres show localized anterior overexpression of *Fgf8* and up-regulation of *Spry1* (arrowhead), indicating expression of functional FGF8 protein (*42*). Bar in (B) is 0.25 mm for (B) and 0.65 mm for (C).

Introducing a second FGF8 source results in duplicate somatosensory barrel fields. These effects on the cortical map could reflect a role for FGF8 in modulating the relative size of neocortical areas along the A/P axis, or a more fundamental role in specifying area identity itself. To distinguish between these possibilities, we introduced a new source of FGF8 into the posterior cortical primordium, i.e., at the opposite pole from the endogenous source. Posterior electroporation of *Fgf8* elicits a partial duplication of S1: New whisker barrels appear ectopically in posterior neocortex (n = 10) (Fig. 5). In some cases, extra barrels form a distorted subfield that merges with the native S1 (Fig. 5, B and C). Most striking, in some

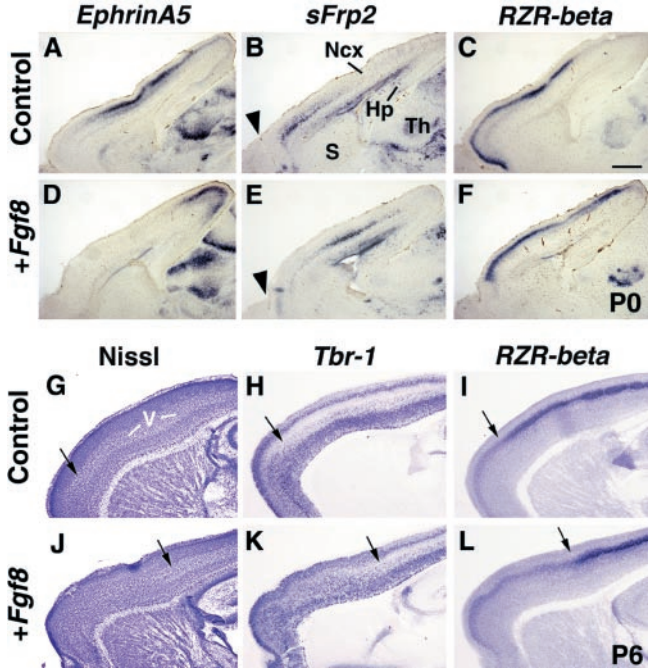

Fig. 2. Anterior overexpression of FGF8 results in a posterior shift of cortical domains. (**A** to **L**) Saggittal sections (anterior to the left) through P0 (A to F) or P6 (G to L) brains processed for in situ hybridization (A to F, H and I, K and L) or Nissl stain (G and J). Each brain was electroporated with *Fgf8* in one hemisphere at E11.5. (D) to (F) and (J) to (L) are sections from the +*Fgf8* hemispheres; (A) to (C) and (G) to (I) are from matched medial-lateral levels in the nonelectroporated (control) hemisphere. In the P0 +*Fgf8* hemisphere (D to F), compared with the control (A to C), domains of *RZR-beta*, *EphrinA5* and *sFrp2* expression are shifted posteriorly by 1 to 1.5 mm, one-quarter to one-third of the total neocortical A/P length [arrowheads in (B) and (E) indicate the frontal pole of the neocortex for reference]. The *EphrinA5* expression domain shrinks as it is shifted back, as if running out of available neocortical territory (D). At P6, the boundary between somatosensory and motor cortex is marked by the anterior limit of a lightly Nissl-stained layer V and by transitions in the expression of *Rzr-beta* and the T-box transcription factor *Tbr-1* [arrows in (G) to (I)]. The somatosensory/motor boundary is shifted posteriorly in an +*Fgf8* hemisphere [arrows in (J) to (L)] by about 1.5 mm (total neocortical length, about 6 mm), and a region displaying the *Tbr-1* and Nissl layer pattern typical of frontal cortex is expanded (K and L). Abbreviations: Hp, hippocampus; Ncx, neocortex; S, striatum; Th, thalamus; V, layer five of neocortex. Bar in (C) is 0.5 mm for (A) to (L).

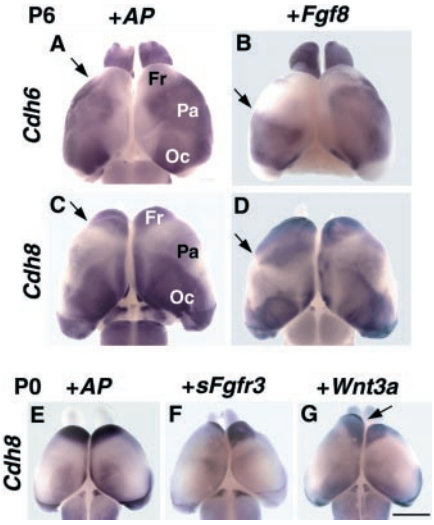

Fig. 3. Expression of *Cdh6* and *8* reveals global shifts in area pattern. (**A** to **G**) Dorsal views of P6 (A to D) or P0 (E to G) brains, anterior to the top. Left hemispheres were electroporated at anterior sites with *AP* (A, C, and E), *Fgf8* (B and D), *sFgfr3* (F), or *Wnt3a* (G); right hemispheres serve as internal controls. In P6 *Fgf8*+ hemispheres, a frontal domain (Fr) marked by low *Cdh6* expression and high *Cdh8* expression is expanded [arrows in (A) to (D)], and a *Cdh6*-high/*Cdh8*-low parietal domain (Pa) is shifted back and shrunken, as is an occipital domain (Oc) that expresses both cadherins. *AP*+ hemispheres show no shifts (A and C). At P0, the left frontal *Cdh8*-high domain is unchanged by *AP* (E), reduced by *sFgfr3* (F), and expanded by *Wnt3a* electroporation (G). WNT3A-induced expansion correlates with an overgrowth of the left frontal pole [arrow in (G)]. Bar in (G) is 2.8 mm for (A) to (D) and 2 mm for (E) to (G).

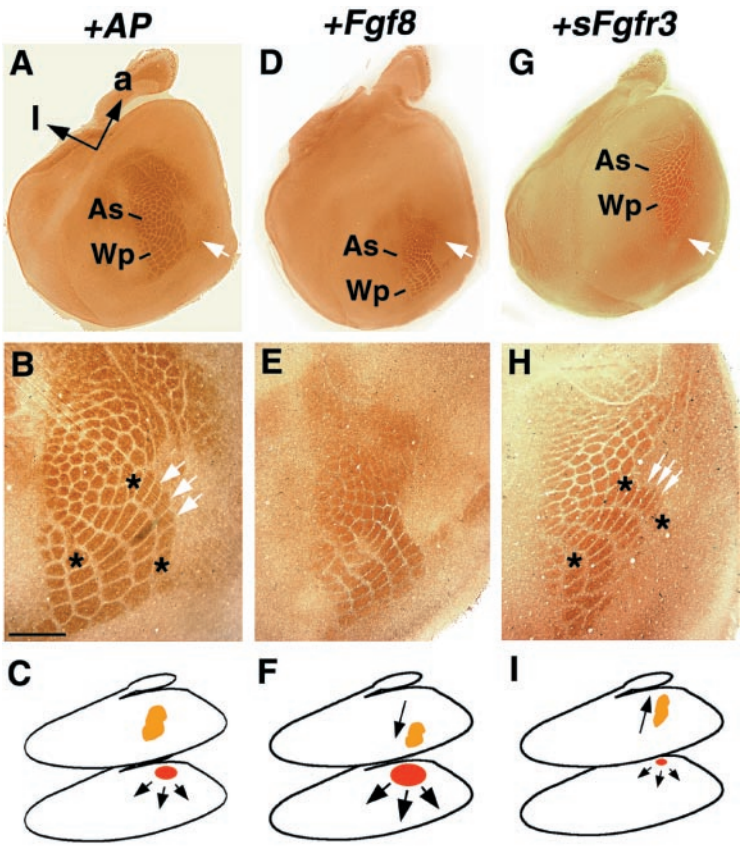

Fig. 4. Anterior electroporation of *Fgf8* or *sFGFR3* causes opposite shifts of the S1 barrel fields. (**A**, **B**, **D**, **E**, **G**, **H**) Tangential sections through layer 4 of flattened P6 cortices processed for cytochrome oxidase (CO) histochemistry. Patches of high CO activity mark individual barrels in S1 (*43*). Anterior (a) and lateral (l) are indicated in (A). White arrows in (A), (D), and (G) mark the midpoint between anterior and posterior poles of the neocortex. (B), (E), and (H) are higher magnification views of (A), (D), and (G). (**C**, **F**, and **I**) A model of FGF8 signaling effects on S1. The whisker pad (Wp) and anterior snout (As) subfields are centrally positioned in an +*AP* cortex (A) with a presumed normal anterior FGF8 source [red oval in (C)]. An augmented FGF8 source (F) pushes the Wp and As fields into the posterior half of the neocortex and compresses them (D and E). Reduction of the source (I) draws the fields into the anterior half of the neocortex (G) and elongates individual Wp barrels along the A/P axis [compare barrels marked by white arrows in (B) and (H)]. The Wp subfield is also skewed and elongated along the A/P axis [compare the relative positions of three barrels marked with asterisks in (B) and (H)]. Bar in (B) is 2.0 mm for (A), (D), and (G), and 0.7 mm for (B), (E), and (H).

animals, a second, entirely separate whisker pad subfield is generated (Fig. 5, A, D, and E). Whereas the native subfield is divided into five curving rows, from A to E, with A most posterior (Fig. 4B and Fig. 5, D and E), in ectopic subfields, the curve and order of the rows appears reversed (Fig. 5, D and E). Thus, a posterior source of FGF8 appears to create a local reversal of A/P positional values in the cortical primordium. A posterior region of the primordium is specified to take on a more anterior identity and form a new, inverted S1 subfield. The most parsimonious interpretation of our results is that an FGF signal specifies positional identity in the cortical primordium, and that the area map distortions caused by our experimental manipulations reflect changes in this specification.

Discussion. We present here direct evidence that a secreted signaling molecule can regulate the neocortical area map and, in particular, that an FGF signal controls patterning along the A/P axis. Patterning along the medial-lateral axis of the cerebral cortex could be regulated by other signaling molecule families. Candidates include epidermal growth factor (EGF) proteins expressed near the lateral boundary of the cortical primordium and shown to regulate expression of the limbic area marker LAMP (*3*, *36*), and BMP and WNT proteins expressed in the medially positioned cortical hem (*9*, *11*, *29*, *37*). Sup-

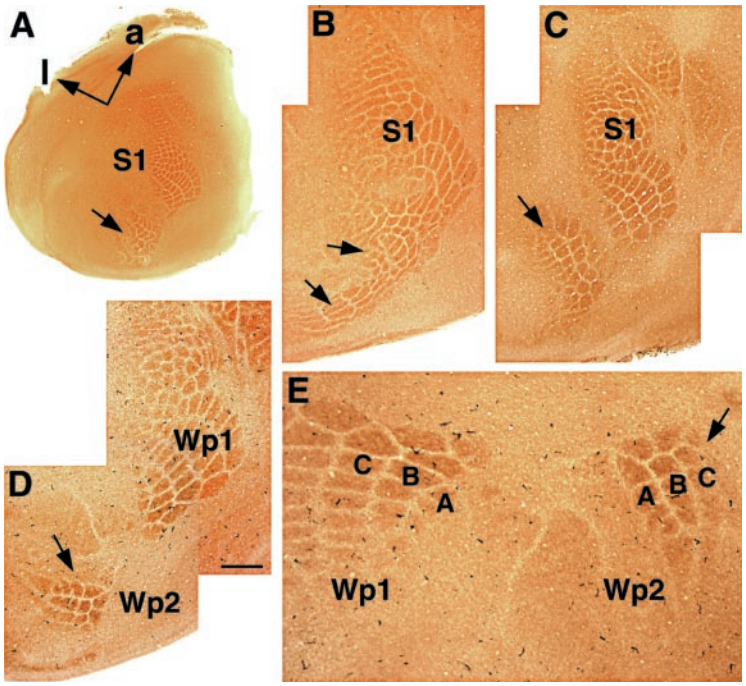

Fig. 5. A posterior source of *Fgf8* generates ectopic S1 barrels. (**A** to **E**) Four flattened cortices analyzed at P6 after electroporation of *Fgf8* into the posterior cortical primordium at E11.5. (E) is a rotated, higher magnification view of (D). Anterior is as indicated in (A) for (A) to (D), and is to the left for (E). Ectopic barrels (A to E, arrows) appear posterior to the native S1, forming subfields that merge with the native S1 (B), partially merge (C), or are entirely separate (A, D, and E). (D and E) A partial second Wp subfield (Wp2), the number and pattern of its barrels indicating rows A, B, and C [compare (E) with Fig. 4B]. The curved fan shape and apparent row order of Wp2 suggest that it is A/P reversed with respect to the native Wp1 (D and E). Bar in (D) is 1.5 mm for (A), 0.6 mm for (B), (C), and (D), and 0.25 mm for (E).

port is therefore growing for a new model of area specification in which patterning of the part of the brain responsible for our higher functions is coordinated by the same basic mechanisms and signaling protein families used to generate patterning in other embryonic organs (*3*–*7*).

Our findings further suggest one type of mechanism by which the area map might be altered in evolution. Area maps in different species share topological features, suggesting broad similarities in patterning mechanism, but they also differ in area position, size, and number (*1*). In primate cortex, for example, multiple visual sensory areas appear to have been added in evolution, each characterized by separate retinotopic maps that show abrupt mirror-image reversals at area boundaries. Our observations suggest that the template of a new area could be generated by a local modulation in signaling by a single growth factor.

References and Notes

1. W. J. H. Nauta, M. Feirtag, *Fundamental Neuroanatomy* (Freeman, New York, 1986).
2. P. Rakic, *Science* **241**, 170 (1988).
3. P. Levitt, M. F. Barbe, K. L. Eagleson, in *Annual Review of Neuroscience*, W. M. Cowan, Ed. (Annual Reviews, Palo Alto, CA, 1997), vol. 20, p. 1.
4. J. L. R. Rubenstein *et al.*, *Cereb. Cortex* **9**, 524 (1999).
5. E. M. Miyashita-Lin *et al.*, *Science* **285**, 906 (1999).
6. K. M. Bishop *et al.*, *Science* **288**, 344 (2000).
7. C. W. Ragsdale, E. A. Grove, *Curr. Opin. Neurobiol.* **11**, 50 (2001).
8. P. H. Crossley, G. R. Martin, *Development* **121**, 439 (1995).
9. Y. Furuta *et al.*, *Development* **124**, 2203 (1997).
10. K. Shimamura, J. L. R. Rubenstein, *Development* **124**, 2709 (1997).
11. E. A. Grove *et al.*, *Development* **125**, 2315 (1998).
12. P. H. Crossley *et al.*, *Nature* **380**, 66 (1996).
13. A. Neubuser *et al.*, *Cell* **90**, 247 (1997).
14. W. Ye *et al.*, *Cell* **93**, 755 (1998).
15. H. Shamim *et al.*, *Development* **126**, 945 (1999).
16. A. S. Tucker *et al.*, *Development* **126**, 51 (1999).
17. M. Heikinheimo *et al.*, *Mech. Dev.* **48**, 129 (1994).
18. C. W. Ragsdale *et al.*, unpublished observations.
19. K. Yasuda *et al.*, *Dev. Growth Differ.* **42**, 203 (2000).
20. S. Agarwala *et al.*, *Science* **291**, 2147 (2001).
21. K. J. Huffman *et al.*, *J. Neurosci* **19**, 9939 (1999).
22. Y. Gitton *et al.*, *J. Neurosci.* **19**, 4889 (1999).
23. M. F. Barbe, P. Levitt, *J. Neurosci.* **11**, 519 (1991).
24. K. Mackarehtschian *et al.*, *Cereb. Cortex* **9**, 601 (1999).
25. S. C. Suzuki *et al.*, *Mol. Cell. Neurosci.* **9**, 433 (1997).
26. C. A. MacArthur *et al.*, *Cell Growth Differ.* **6**, 817 (1995).
27. S. M. Lee *et al.*, *Development* **124**, 959 (1997).
28. J. Xu *et al.*, *Development* **127**, 1833 (2000).
29. S. M. Lee *et al.*, *Development* **127**, 457 (2000).
30. A. Chellaiah *et al.*, *J. Biol. Chem.* **274**, 34785 (1999).
31. C. A. MacArthur *et al.*, *Development* **121**, 3603 (1995).
32. T. Fukuchi-Shimogori, E. A. Grove, unpublished observations.
33. T. A. Woolsey, H. Van der Loos, *Brain Res.* **17**, 205 (1970).
34. H. Van der Loos, T. A. Woolsey, *Science* **179**, 395 (1973).
35. K. F. Jensen, H. P. Killackey, *J. Neurosci.* **7**, 3529 (1987).
36. R. T. Ferri, P. Levitt, *Development* **121**, 1151 (1995).
37. J. Galceran *et al.*, *Development* **127**, 469 (2000).
38. Timed-pregnant CD-1 mice were obtained from the University of Chicago Cancer Research Center Transgenic Facility. Noon of the day on which a vaginal plug is seen is termed E0.5. Animal care was according to institutional guidelines.
39. The expression vector backbone was pEF1/Myc-His C (Invitrogen), with gene expression driven from the human elongation factor 1α promoter enhancer. A 2.2-kb fragment between Pvu II sites containing neomycin and SV40 elements was removed to reduce plasmid size, generating pEFX (*20*). Complementary DNAs encoding mouse FGF8 isoform b, mouse WNT3a, human placental alkaline phosphatase (AP), or a truncated, soluble human FGFR3c (sFGFR3) were inserted into pEFX. *sFGFR3* was generated with 5′-GCCATGGGCGCCCCTGCCTGCGCCCTCGC-3′ and 3′-TCGGGGGGGTTCTTTCCGGACCCGAGGATT-5′ polymerase chain reaction primers and encodes the extracellular portion of FGFR3c.
40. Analysis of 295 *AP*-electroporated cortical hemispheres with gene expression, morphological, cell proliferation, or cell death assays indicates that electroporation under our conditions does not itself disrupt neocortical development.
41. G. Minowada *et al.*, *Development* **126**, 4465 (1999).
42. Most electroporated brains required analysis at P0 or P6, several days after transient ectopic gene expression could be directly detected. To determine the frequency of effective gene transfection, several litters were electroporated at E11.5 with *Fgf8* or *AP* plasmids and harvested 48 hours later. Half of the surviving embryos in each litter showed strong transgene expression (31/60). Consistent with this observation, shifts in area domains (Figs. 2 to 4) were seen at P0 or P6 in about one-half of the mice electroporated with *Fgf8* or *sFGFR3* at E11.5 (n = 56/108 with 52 brains showing no shifts). Shifts were invariably consistent, i.e., in the posterior direction for anterior FGF8 overexpression and in the anterior direction for presumed FGF inhibition. No shifts were seen in mice electroporated with the *AP* control plasmid (n = 0/51). Ectopic S1 barrels (Fig. 5) appeared in 10/37 P6 brains after posterior electroporation of *Fgf8*. This lower frequency of effect may be due to the greater difficulty of successful posterior electroporation. Ectopic S1 barrels were not seen after posterior electroporation of AP (n = 0/24).
43. M. T. Wong-Riley, C. Welt, *Proc. Natl. Acad. Sci. U.S.A.* **77**, 2333 (1980).

44. We thank S. Agarwala, S. Assimacopoulos, P. Mason, C. W. Ragsdale, T. Sanders, and C. S. Wellek for discussion and technical help and advice and C. MacArthur, A. McMahon, G. Martin, S. McConnell, M. Donoghue, M. Takeichi, M. J. Hayman, and A. Rattner for cDNAs. Supported by NIH and the March of Dimes Birth Defects Foundation.

10 July 2001; accepted 10 September 2001
Published online 20 September 2001;
10.1126/science.1064252
Include this information when citing this paper.

Universality and Scaling in the Disordering of a Smectic Liquid Crystal

Tommaso Bellini,[1,2] Leo Radzihovsky,[1] John Toner,[3] Noel A. Clark[1]

We present experimental and theoretical studies of the effects of quenched disorder on one-dimensional crystal ordering in three dimensions. This fragile smectic liquid crystal layering, the material with the simplest positional order, is also the most easily deformed periodic structure and is, therefore, profoundly affected by disorder, introduced here by confinement in silica aerogel. Theory and experiment combine to characterize this system to an extraordinary degree, their close accord producing a coherent picture: crystal ordering is lost, giving way to extended short-range correlations that exhibit universal structure and scaling, anomalous layer elasticity, and glassy dynamics.

A major part of condensed matter physics is directed toward understanding the effects of disorder, defects, and impurities, which are responsible for many materials properties and failures. Theoretical models, which systematically introduce disorder into well-understood clean systems, reveal rich and complex phenomena that challenge and broaden our understanding of statistical physics. The effects of disorder can be dramatic, destabilizing phases (*1*–*3*) and producing new ones (*4*–*7*), as well as altering otherwise "universal" behavior near transitions (*8*, *9*). Liquid crystals (LCs), by virtue of their fluidity, their intrinsically soft elasticity, and their experimental accessibility, offer exceptional opportunites for the study of the structural and dynamical effects of quenched disorder, which can be readily introduced, for example, by confinement within appropriate random porous media. Such studies are also of interest in connection with composite electro-optic materials in which randomness is imposed on the LC, for example, by introduction of polymer or nanoparticles (*10*). The starting point for developing a theoretical description of LCs confined in a random environment is to study the effects of weak random point forces and torques on the LC order, an idealized disordering mechanism that affects molecular location and orientation in random ways but occupies as little physical space as possible. This situation can, in fact, be approached in the laboratory by incorporating the LC into the connected void space of an aerogel, a highly

[1]Department of Physics, University of Colorado, Boulder, CO 80309, USA. [2]INFM, Dipartimento di Chimica e Biochimica Medica, Universitá di Milano, Milano, Italy. [3]Department of Physics, Materials Science Institute, and Institute of Theoretical Science, University of Oregon, Eugene, OR 97403, USA.